PROCEEDINGS OF SCIENCE

Revealing similarity in multihadron production in hadronic and nuclear collisions

Aditya Nath Mishra*
Indian Institute of Technology Indore, Indore-452017, India
E-mail: amishra@cern.ch

Raghunath Sahoo
Indian Institute of Technology Indore, Indore-452017, India
E-mail: Raghunath.Sahoo@cern.ch

Edward K. G. Sarkisyan
Department of Physics, CERN, 1211 Geneva 23, Switzerland and
Department of Physics, The University of Texas at Arlington, Arlington, TX 76019, USA
E-mail: sedward@cern.ch

Alexander S. Sakharov
Department of Physics, CERN, 1211 Geneva 23, Switzerland
Department of Physics, New York University, New York, NY 10003, USA and
Physics Department, Manhattan College, New York, NY 10471, USA
E-mail: Alexandre.Sakharov@cern.ch

Universality of multihadron production in AA and hadronic interactions is studied using collision energy and centrality dependencies of the measured charged particle mean multiplicity. The study uses the framework of an effective-energy approach combining the constituent quark picture and Landau relativistic hydrodynamics and relating hadronic and nuclear collisions. The energy dependence of the multiplicity and the pseudorapidity density of head-on AA collisions are well reproduced. The multiplicity centrality dependence reveals a new scaling between the measured and estimated pseudorapidity spectra. Using this scaling, called the energy balanced limiting fragmentation scaling, all centrality spectra are described. This elucidates the difference in centrality dependence of multiplicity at RHIC and LHC and also the RHIC midrapidity density vs multiplicity. A new regime in AA collisions is indicated at $\sim$1 TeV. Predictions are made for the multiplicities to be measured in pp and AA collisions at LHC.

7th International Conference on Physics and Astrophysics of Quark Gluon Plasma
1-5 February , 2015
Kolkata, India

*Speaker.

PoS(ICPAQGP2015)052

1. Multiparticle production in high-energy particle and nuclear collisions attracts high interest, as, on the one hand, the observables measured first in high-energy collisions, namely multiplicity and transverse energy, are immediate characteristics of this process and bring important information on the underlying dynamics of strong interactions, while on the other hand, this process still eludes its complete understanding [1]. Recently, the universality of multiparticle production in nucleus-nucleus and hadron-hadron collisions has been reported exploiting the effective energy concept [2] employed for the data interpreted in terms of the quark participant dissipating energy approach [3, 4]. This approach combines the constituent quark picture together with Landau relativistic hydrodynamics and interrelates different types of collisions. In this report, based on [5], we extend the previous studies of the charged particle mean multiplicity [3, 4] of nucleus-nucleus collisions up to the LHC energies in the framework of the quark participant dissipating effective-energy approach. We introduce a new scaling, called the energy balanced limiting fragmentation scaling, which allows to describe the pseudorapidity density spectra independent of the centrality of collisions.

2. The constituent quark participant effective-energy approach quantifies the process of particle production in terms of the amount of energy deposited by interacting constituent quark participants inside the small Lorentz-contracted volume formed at the early stage of a collision. The whole process of a collision is then represented as the expansion and the subsequent break-up into particles from an initial state. This approach resembles the Landau phenomenological hydrodynamic approach of multiparticle production in relativistic particle interactions [6], which was found to be in a good agreement with the multiplicity data in particle and nuclear collisions in the wide energy range [7]. In the picture proposed here, the Landau hydrodynamics is combined with the constituent quark model [8, 9]. This makes the secondary particle production to be basically driven by the amount of the initial effective energy deposited by participants – quarks or nucleons, into the Lorentz contracted overlap region. In $pp/\bar{p}p$ collisions, a single constituent quark from each nucleon is considered to take part in a collision and rest are treated as spectators. The spectator quarks do not participate in secondary particle production while resulting into formation of leading particles carry away a significant part of the collision energy. Thus, the effective energy for the production of secondary particles is the energy of interaction of a single quark pair, *i.e.*, 1/3 of the entire nucleon energy. Contrary, in the head-on heavy-ion collisions, the participating nucleons are considered colliding by all three constituent quarks from each nucleon which makes the whole energy of the colliding nucleons (participants) available for secondary particle production. Within this picture, one expects that bulk observables measured in head-on heavy-ion collisions at the c.m. energy per nucleon, $\sqrt{s_{NN}}$, to be similar to those from $pp/\bar{p}p$ collisions but at a three times larger c.m. energy, *i.e.*, at $\sqrt{s_{pp}} \simeq 3\sqrt{s_{NN}}$. Such a universality is found to correctly predict [3] the value of the midrapidity density in pp interactions measured at the TeV LHC energies [10]. For recent discussion on the universality of hadroproduction up to LHC energies, see [11].

Combining the above discussed ingredients, one obtains the relationship between charged particle rapidity densities, $\rho(\eta) = (2/N_{\rm part})dN_{\rm ch}/d\eta$ at midrapidity ($\eta \approx 0$) in heavy-ion and in $pp/\bar{p}p$ collisions:

$$\frac{\rho(0)}{\rho_{pp}(0)} = \frac{2N_{\rm ch}}{N_{\rm part}N_{\rm ch}^{pp}}\sqrt{\frac{L_{pp}}{L_{NN}}}, \quad \sqrt{s_{pp}} = 3\sqrt{s_{NN}}\,. \tag{1}$$

In Eq.(1), the relation of the pseudorapidity density and the mean multiplicity is applied in its Gaussian form as obtained in Landau hydrodynamics. The factor L is defined as $L = \ln(\sqrt{s}/2m)$. According to the approach considered, m is the proton mass, m_p, in nucleus-nucleus collisions and the constituent quark mass in $pp/\bar{p}p$ collisions which is set to $\frac{1}{3}m_p$. $N_{\rm ch}$ and $N_{\rm ch}^{pp}$ are the mean multiplicities in nucleus-nucleus and nucleon-nucleon collisions, respectively, and $N_{\rm part}$ is the number of participants. Solving Eq. (1) for the multiplicity $N_{\rm ch}$ at a given rapidity density $\rho(0)$ at $\sqrt{s_{NN}}$, and the rapidity density $\rho_{pp}(0)$ and the multiplicity $N_{\rm ch}^{pp}$ at $3\sqrt{s_{NN}}$, one finds:

$$\frac{2N_{\rm ch}}{N_{\rm part}} = N_{\rm ch}^{pp}\,\frac{\rho(0)}{\rho_{pp}(0)}\sqrt{1-\frac{2\ln 3}{\ln\left(4.5\sqrt{s_{NN}}/m_p\right)}}\,,\quad \sqrt{s_{NN}} = \sqrt{s_{pp}}/3\,. \tag{2}$$

Further development [2], as outlined below, treats this dependence in terms of centrality. The centrality is considered to characterize the degree of overlapping of the volumes of the two colliding nuclei, determined by the impact parameter. The centrality is closely related to the number of nucleon participants determined using a Monte Carlo Glauber calculations so that the largest number of participants contribute to the most central heavy-ion collisions. Hence the centrality is related to the energy released in the collisions, *i.e.*, the effective energy, ε_{NN}, which, in the framework of the proposed approach, can be defined as a fraction of the c.m. energy available in a collision according to the centrality, α:

$$\varepsilon_{NN} = \sqrt{s_{NN}}(1-\alpha). \tag{3}$$

Conventionally, the data are divided into classes of centrality, or centrality intervals, so that α is the average centrality for the centrality interval, *e.g.* $\alpha = 0.05$ for the 0–10% centrality interval. Then, for the effective c.m. energy ε_{NN}, Eq. (2) reads:

$$\frac{2N_{\rm ch}}{N_{\rm part}} = N_{\rm ch}^{pp}\,\frac{\rho(0)}{\rho_{pp}(0)}\sqrt{1-\frac{2\ln 3}{\ln\left(4.5\,\varepsilon_{NN}/m_p\right)}}\,,\quad \varepsilon_{NN} = \sqrt{s_{pp}}/3\,, \tag{4}$$

where $\rho(0)$ is the midrapidity density in central AA collisions measured at $\sqrt{s_{NN}} = \varepsilon_{NN}$.

In fact, each of the scalings described by Eqs.(2) and (3) regulates a particular physics ingredient used in the modeling of our approach. Namely, the scaling introduced by Eq.(2) embeds the constituent quark model, which leads to establishing a similarity between hadronic and nuclear collisions, while the scaling driven by Eq.(3) is appealed to define the energy budget effectively retained for multiparticle production in the most central collisions to determine the variables obtained from centrality data.

3. The c.m. energy dependence of the multiplicity measured in head-on nucleus-nucleus collisions (solid symbols) is shown in Figure 1. We fit the head-on data by the "hybrid" fit function (solid line), similar to the successful hybrid fits considered by us earlier for the charged particle midrapidity density and the midrapidity transverse energy density [2].The motivation behind hybrid function is that the logarithmic dependence is considered to characterize the fragmentation source(s) while the power-law behaviour is believed to come from the gluon-gluon interactions [12]; for review, see [13]. In addition to the hybrid fit, we show the $\log^2(s_{NN})$-fit [3, 4] up to

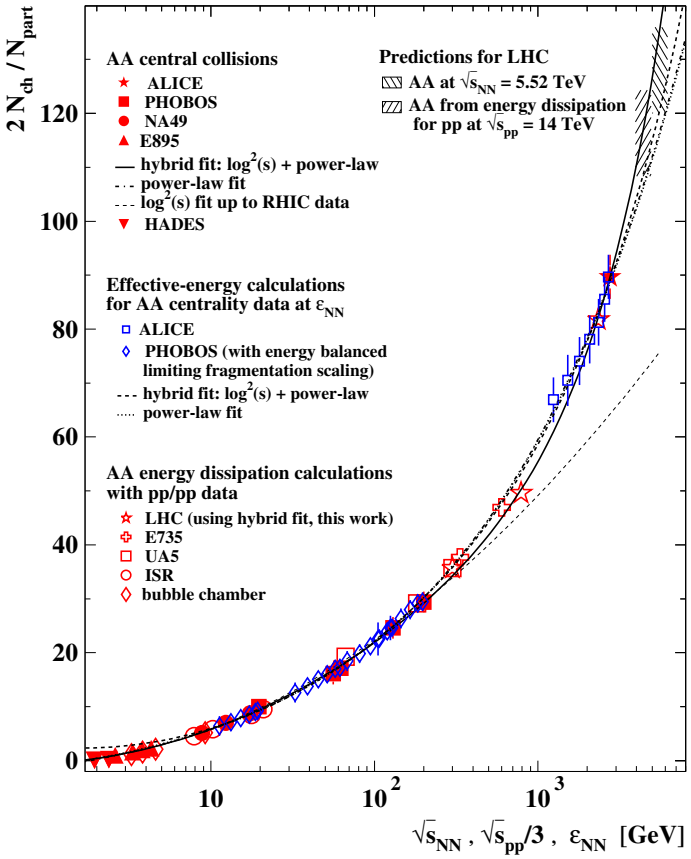

Figure 1: The energy dependence of the charged particle mean multiplicity per participant pair in nucleus-nucleus collisions. The hybrid fits are: $-0.577+0.394\ln(s_{NN})+0.213\ln^2(s_{NN})+0.005s_{NN}^{0.551}$ and $2.45-1.06\ln(\varepsilon_{NN})+1.04\ln^2(\varepsilon_{NN})+0.082\,\varepsilon_{NN}^{0.744}$, for head-on and the centrality data, correspondingly.

the top RHIC energy (thin dashed line) and the power-law fit for the entire energy range (dashed-dotted line); for the functional form, see [5]. One can see that the power-law fit well describes the data and is almost indistinguishable from the hybrid fit up to the LHC data. Some minor deviation between the two fits can be seen in the range from the top RHIC energy to the LHC energy. Meanwhile, the 2nd-order log-polynomial lies below the data at $\sqrt{s_{NN}} > 200$ GeV. This observation supports a possible transition to a new regime in heavy-ion collisions at $\sqrt{s_{NN}}$ at about 1 TeV, as indicated [2] in the studies of midrapidity pseudorapidity particle and transverse energy densities.

Addressing now Eq. (2), the mean multiplicity per participant pair, $N_{\rm ch}/(N_{\rm part}/2)$, for nucleus-nucleus interactions is calculated (large open symbols) using the $pp/\bar{p}p$ measurements. The rapidity density $\rho_{pp}(0)$ and the multiplicity $N_{\rm ch}^{pp}$ are taken from the existing data [11] or, where not available, calculated using the corresponding experimental fits[1]. The $\rho(0)$ values are as well taken from the measurements in central heavy-ion collisions wherever available, while for the non-existing data the hybrid fit is used [2]. One can see that the calculated $N_{\rm ch}/(0.5N_{\rm part})$ values follow

[1]The hybrid fit to $2N_{\rm ch}/N_{\rm part}$ in head-on heavy-ion collisions is taken from Fig. 1, while $\rho_{pp}(0)$ is calculated using the linear-log fit $\rho_{pp}(0) = -0.308+0.276\ln(s_{pp})$ [14] and the power-law fit by CMS [15], $\rho_{pp}(0) = -0.402+s_{pp}^{0.101}$, at $\sqrt{s_{pp}} \leq 53$ GeV and at $\sqrt{s_{pp}} > 53$ GeV, respectively.

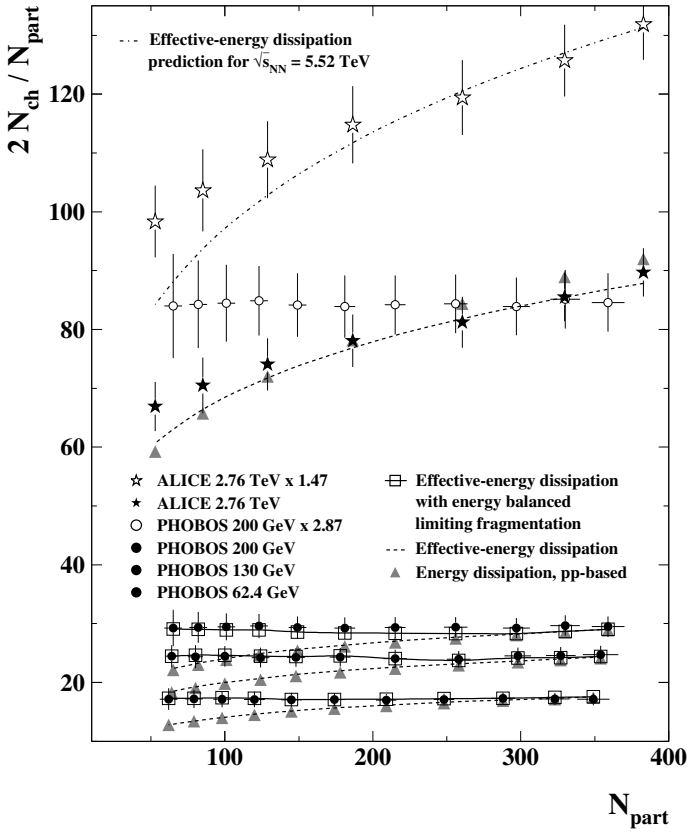

Figure 2: The charged particle mean multiplicity per participant pair as a function of the number of participants, $N_{\rm part}$.

the nuclear measurements at $\sqrt{s_{NN}}$ from a few GeV up to the TeV LHC energy pointing to the universality of the multiparticle production process in different types of collisions.

Solving Eq. (2) for the mean multiplicity in pp collisions, $N_{\rm ch}^{pp}$, we estimate its values for $\sqrt{s_{pp}} >$ 2 TeV to be about 48 at $\sqrt{s_{pp}} = 2.36$ TeV, 69 at 7 TeV, and 81 at 14 TeV with 5 to 10% uncertainties. No change in the multihadron production in pp interactions up to the top LHC energy in contrast to a new regime possibly occurred at $\sqrt{s_{NN}} \approx 1$ TeV in heavy-ion collisions. The quark-participant energy-dissipation approach predictions on $N_{\rm ch}^{pp}$ at $\sqrt{s_{pp}} > 2$ TeV are found to follow well the hybrid (or power-law) fit function to the measurements made at $\sqrt{s_{pp}} \leq 1.8$ TeV. This and the above indication of no change in hadroproduction in pp collisions as soon at TeV energies are in an agreement with the successful prediction [3] seems within the dissipating energy approach only made for the midrapidity density in pp collisions at $\sqrt{s_{pp}} = 7$ TeV [10].

4. In this section, we address the mean multiplicity centrality dependence from heavy-ion experiments to be described by Eq. (4) similar to the midrapidity pseudorapidity density in [2]. In Fig. 2, we show the $N_{\rm part}$-dependence of $N_{\rm ch}/(N_{\rm part}/2)$. The data are taken from the measurements by PHOBOS experiment at RHIC [16] and by ALICE experiment at LHC [17, 18]. The PHOBOS data at $\sqrt{s_{NN}} = 200$ GeV multiplied by 2.87 are also shown to allow comparison with the LHC data and the current calculations. The solid triangles show the estimations using Eq. (4). According to

the consideration here, $\rho(0)$ is taken at $\sqrt{s_{NN}} = \varepsilon_{NN}$, and $\rho_{pp}(0)$ and $N_{\rm ch}^{pp}$ are taken at $\sqrt{s_{pp}} = 3\,\varepsilon_{NN}$. One can see that the calculations, which are driven by the centrality-defined effective c.m. energy ε_{NN}, well reproduce the LHC data. However, a significant difference between the calculations and the measurements is visible for medium centralities at RHIC energies. These observations are contradicting the centrality independent multiplicity measured at RHIC energies. In Fig. 2, the above- obtained hybrid fit to c.m. energy dependent *head-on* collision data, is applied to the *centrality* measurements at $\sqrt{s_{NN}} = \varepsilon_{NN}$. The observations made for the calculations are valid here as well. To clarify on the observed differences, in the following sections the pseudorapidity density distributions are investigated in the context of the approach considered here.

5. In Fig. 3, the charged particle pseudorapidity density distributions per participants pair measured in head-on or very central AuAu collisions by PHOBOS experiment at the RHIC at $\sqrt{s_{NN}} =$ 19.6, 62,4 and 200 GeV [16] and in central PbPb collisions by ALICE experiment at the LHC at $\sqrt{s_{NN}} = 2.76$ TeV [17] are shown. Along with the heavy-ion data, the charged particle pseudorapidity density distributions from $pp/\bar{p}p$ interactions are also shown as measured by different experiments. The data are taken at the c.m. energies $\sqrt{s_{pp}} \approx 3\sqrt{s_{NN}}$ or $3\,\varepsilon_{NN}$.

Within the considered model of constituent quarks and the Gaussian form of the pseudorapidity distribution in Landau hydrodynamics, the relationship between the pseudorapidity density distributions $\rho(\eta)$ and $\rho_{pp}(\eta)$ reads

$$\frac{\rho(\eta)}{\rho_{pp}(\eta)} = \frac{2N_{\rm ch}}{N_{\rm part}N_{\rm ch}^{pp}}\sqrt{1+\frac{2\ln 3}{L_{NN}}}\,\exp\left[\frac{-\eta^2}{L_{NN}\,(2+L_{NN}/\ln 3)}\right]. \tag{5}$$

Here, all variables are defined in a way it is done in Eq. (1) taking into account the constituent quark scaling of the c.m. energy as one relates $pp/\bar{p}p$ interactions to central heavy-ion collisions. Using Eq. (5), the heavy-ion distributions are calculated based on the $\rho_{pp}(\eta)$ spectra shown in Fig. 3 (solid symbols) One can see that the calculations are in very good agreement with the measurements. Minor deviations are due to some mismatch between $\sqrt{s_{pp}}$ and $3\sqrt{s_{NN}}$ (or $3\,\varepsilon_{NN}$) and due to a slight non-centrality; this is especially visible at $\sqrt{s_{NN}} = 19.6$ GeV where the energy mismatch is of a largest fraction. To note is how well the constituent quark energy dissipation picture allows to reproduce the pseudorapidity density distributions from heavy-ion interactions in the full-η range in the $\sqrt{s_{NN}}$ range spanning over more than two orders of magnitude. Remarkably, the pseudorapidity density distributions, measured in $pp/\bar{p}p$ collisions, despite being above those measured in heavy-ion collisions at 19.6 GeV or, on the contrary, lying far below the heavy-ion data from the LHC almost in the full-η range, equally well reproduce the heavy-ion data as soon as being recalculated within the participant energy dissipation approach. Interestingly, for the calculations at the LHC energies, one uses the pp measurements from the three different experiments, which nevertheless well reproduce the heavy-ion data as soon as all the pp data are combined for the calculations. Some slight deviation in the negative-η region is due to some asymmetry in the ALICE data.

Let us now address peripheral collisions to clarify on the deviation in centrality dependence between the data and the calculations as it is observed in Fig 2. In Fig. 4(a) the distribution $\rho(\eta)$ measured [16] in AuAu collisions by PHOBOS experiment at $\sqrt{s_{NN}} = 130$ GeV at 45-50% cen-

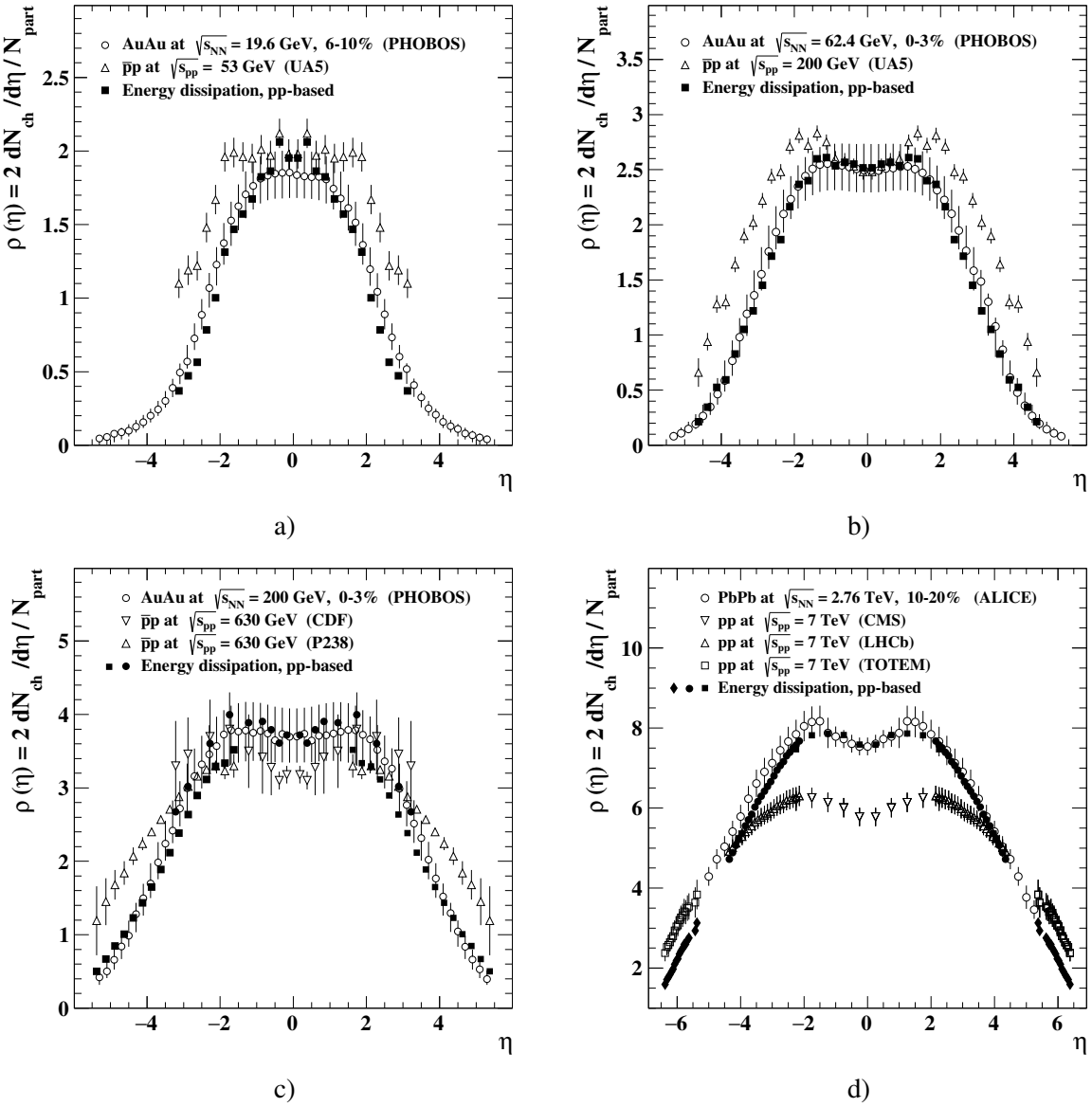

Figure 3: The pseudorapidity distributions of charged particle pseudorapidity density measured in $pp/\bar{p}p$ and head-on or very central heavy-ion collisions compared to the distributions calculated in the framework of the enerrgy-dissipation approach.

trality, $\alpha = 0.475$, is shown along with the $\rho_{pp}(0)$ distribution measured in $\bar{p}p$ collisions by UA5 experiment at $\sqrt{s_{pp}} = 200$ GeV [19], *i.e.*, at $\sqrt{s_{pp}} \approx 3\,\varepsilon_{NN}$ according to the approach considered.

Applying Eq. (5), we calculate the $\rho(\eta)$ spectrum which is shown in Fig. 4(a) by solid squares. The calculations agree well with the measurements in the central-η region while fall below the data outside this region. This finding shows that in non-central collisions, the calculations, reproduce well the pseudorapidity density around the midrapidity while underestimate the mean multiplicity.

To clarify on the features obtained, the following comments are made. In the picture proposed here, the global observables are defined by the energy of the participating constituent quarks

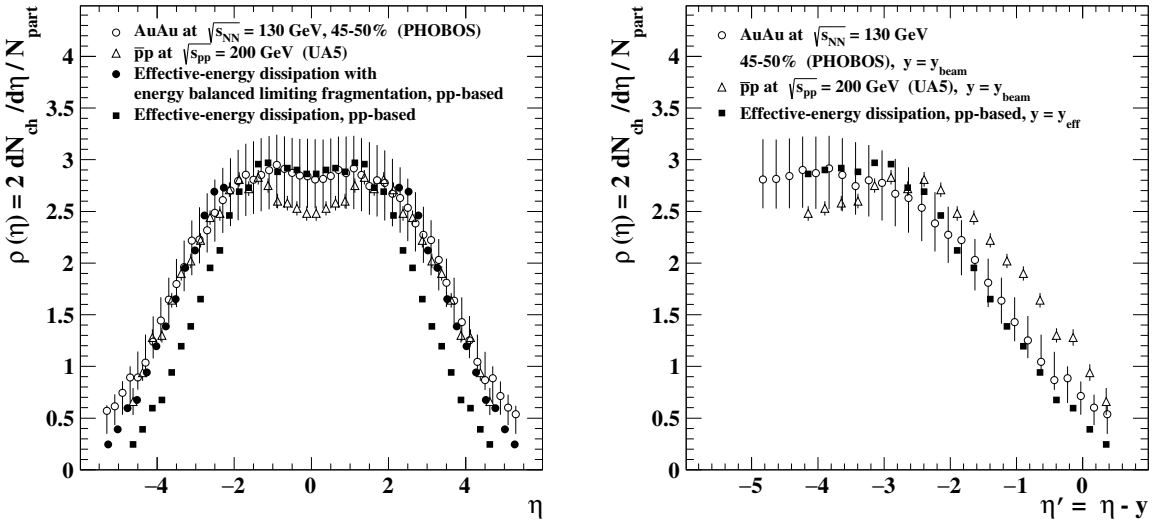

Figure 4: (a) The charged particle pseudorapidity density per participant pair as a function of pseudorapidity. The solid squares show the distribution calculated from Eq. (5) by using the UA5 $\bar{p}p$ data at $\sqrt{s_{pp}} \approx 3\,\varepsilon_{NN}$ (see Eq. (3) for the definition of ε_{NN}). The solid circles show the beyond-midrapidity part obtained from the calculations using the energy balanced limiting fragmentation scaling, i.e. under the shift $\eta \to \eta - \ln(\varepsilon_{NN}/\sqrt{s_{NN}})$. The negative-$\eta$ data points for $\bar{p}p$ interactions are the reflections of the measurements taken in the positive-η region. (b) Same as (a) but the measured distributions of AuAu and $\bar{p}p$ collisions are shifted by the beam rapidity, $\eta' = \eta - y_{\rm beam}$, with $y_{\rm beam} = \ln(\sqrt{s}/m_p)$, where s is, correspondingly, s_{NN} or s_{pp}, and the calculated distribution is shifted to $\eta' = \eta - y_{\rm eff}$ with $y_{\rm eff} = \ln(\varepsilon_{NN}/m_p)$. The distribution measured in AuAu collisions and the calculated distribution coincide in the fragmentation region, when being shifted by $y_{\rm beam}$ for AuAu data and by $y_{\rm eff}$ for the calculations, that represents the energy balanced limiting fragmentation scaling.

pumped into the overlapped area of the colliding nuclei. Hence, the bulk production is driven by the initial energy deposited at zero time at rapidity $\eta = 0$, similar to the Landau hydrodynamics. Then, as it is expected the *about-midrapidity* pseudorapidity density is well reproduced for *all types* of nuclear collisions, from the most central to peripheral ones. As shown in [2], similarly, the centrality dependence of the transverse energy density at midrapidity is well reproduced by the calculations and complements the head-on data c.m. energy dependence within the dissipating effective-energy picture.

From Fig. 4(a), one can see that the calculated distribution $\rho(\eta)$ is narrower than that of the data. The narrowness of the calculated distribution with respect to the measured one is explained by a smaller value of ε_{NN} compared to the value of the collision energy $\sqrt{s_{NN}}$, while the calculations in Eq. (5) are made with the the multiplicity $N_{\rm ch}$ taken from the most central nucleus-nucleus collisions at the c.m. energy equal to ε_{NN}.

6. It is established that in different types of interactions at high enough energies, the pseudorapidity density spectra at different c.m. energies become similar in the fragmentation region, *i.e.*, are independent of a projectile state, in the beam (or target) rest frame for the same type of

colliding objects, *i.e.* been considered as a function of $\eta' = \eta - y_{\rm beam}$, where $y_{\rm beam} = \ln(\sqrt{s_{NN}}/m_p)$ is the beam rapidity [1, 7]. This observation obeys a hypothesis of the limiting fragmentation scaling [20].

Considering the limiting fragmentation hypothesis is applied within the effective-energy approach, one expects the limiting fragmentation scaling of the distribution $\rho(\eta)$ measured at $\sqrt{s_{NN}}$ to be similar to that of the calculated distribution but taken at the effective energy ε_{NN}. Note that the limiting fragmentation phenomenon, though been expected as a universal phenomenon for the Gaussian form of $\rho(\eta)$ [7, 21, 22], naturally arises in Landau hydrodynamics [6].

In Fig. 4(b), the limiting fragmentation hypothesis is shown being applied to both the measured and the calculated pseudorapidity density distributions $\rho(\eta)$ from Fig. 4(a), respectively, using the c.m. energy and the effective energy. Therefore, the measured distribution $\rho(\eta)$ is shifted by the beam rapidity, $y_{\rm beam}$, while the calculated distribution from Eq. (5) is shifted by $y_{\rm eff} = \ln(\varepsilon_{NN}/m_p)$ and becomes a function of $\eta' = \eta - y_{\rm eff}$. One can see that the measured distribution $\rho(\eta')$ of non-central heavy-ion collisions agrees well with the calculated $\rho(\eta')$ distribution, as expected. This finding points to a new energy scaling revealed by using the participant effective-energy approach. In analogy with the limiting fragmentation scaling, we call the observed scaling the *energy balanced* limiting fragmentation scaling. Due to this scaling, the calculated pseudorapidity density is getting corrected outside the central-η region accordingly.

To this end, in Fig. 4(a), the calculated distribution $\rho(\eta)$ is shifted by the difference $(y_{\rm eff} - y_{\rm beam})$ in this region: $\eta \to \eta - \ln(\varepsilon_{NN}/\sqrt{s_{NN}})$, or, using the effective energy definition, Eq. (3), $\eta \to \eta - \ln(1-\alpha)$. This shift of the calculated $\rho(\eta)$ is shown by solid circles in Fig. 4(a). The shift adds the needed *energy balanced* ingredient to the calculations providing the description of the measured pseudorapidity density distribution in the full-η range in non-central heavy-ion collision. It is clear that in head-on or very central collisions, α approaches zero what makes the shift negligible, in order to reproduce the data (cf. Fig. 3).

This finding allows to obtain $N_{\rm ch}$ within the quark participant dissipating effective-energy approach. Namely, the difference between the two $N_{\rm ch}$ values, one obtained by integrating the calculated pseudorapidity density distribution from Eq. (5), and another one of the same distribution but being shifted to the left by $\ln(1-\alpha)$, is added to the $N_{\rm ch}$ value obtained from Eq. (4). Where no pseudorapidity density distributions are available in $pp/\bar{p}p$ measurements at $\sqrt{s_{pp}} = 3\,\varepsilon_{NN}$, the energy balanced limiting fragmentation scaling is applied to reproduce the calculated $\rho(\eta)$: the measured distribution from a non-central heavy-ion collision is shifted by $(y_{\rm beam} - y_{\rm eff})$, *i.e.* $\eta \to \eta + \ln(1-\alpha)$. Then $N_{\rm ch}$ is calculated as above, by adding the difference between the integral from the obtained shifted distribution and the measured multiplicity in this non-central heavy-ion collision to the calculation of Eq. (4).

Using this ansatz, the values of $N_{\rm ch}$ are calculated for each centrality for the RHIC measurements. The calculations are shown by open squares in Fig. 2. One can see that now the calculations well reproduce the measurements from RHIC, with no deficit in non-central collisions.

The energy balanced limiting fragmentation scaling provides an explanation of the "puzzle" between the centrality independence of the $N_{\rm part}$-normalized mean multiplicity and the monotonic decrease of the normalized midrapidity pseudorapidity density with the centrality, as observed at RHIC. As shown above, the pseudorapidity density at midrapidity is determined by the effective energy of *centrally* colliding nucleon participants. However, the multiplicity gets additional con-

tribution from beyond the midrapidity. In the context of the picture proposed here, this contribution is due to the balance between the collision c.m. energy shared by all nucleons of colliding nuclei and the centrality-defined effective energy of the interacting participants. This contribution can be directly estimated by the energy balanced limiting fragmentation scaling, here introduced.

From Fig. 2 one can conclude that, in contrast to the RHIC measurements, almost no additional contribution is needed for the participant dissipating energy calculations of Eq. (4) in order to describe the LHC mean multiplicity data. Given the multiplicity measurements at the LHC are well reproduced without the energy balanced additional contribution to be included, one concludes that in heavy-ions collisions at the LHC at TeV energies the multihadron production obeys a head-on collision regime, at least for the centrality intervals measured so far. This points to apparently different regimes of hadroproduction in heavy-ion collisions up to $\sqrt{s_{NN}}$ of a few hundred GeV energies and in those happenning at TeV energies.

7. Given the obtained agreement between the data and the calculations and considering the similarity put forward for ε_{NN} and $\sqrt{s_{NN}}$, one would expect the measured centrality data at ε_{NN} to follow the $\sqrt{s_{NN}}$ dependence of the mean multiplicity in the most central nuclear collisions. In Fig. 1, the measurements of the charged particle mean multiplicity of *head-on* nuclear collisions are added by the *centrality* measurements by PHOBOS [16] and ALICE [17, 18] experiments (Fig. 2) where the centrality data are plotted as a function of ε_{NN}. Due to the above finding of the energy balanced limiting fragmentation scaling, leading to the lack of centrality dependence of the mean multiplicity at RHIC energies, these data are plotted by subtracting the energy balanced contribution. In addition, the centrality data at $\sqrt{s_{NN}} = 19.6$ GeV are given while are not shown in Fig. 2. From Fig. 1, one concludes that the centrality data effective-energy dependence complement the data on the head-on collision c.m. energy behaviour.

To better trace the similarity between the head-on collision and centrality data, we fit the centrality data ε_{NN}-dependence by the hybrid and the power-law fits given in Fig. 1. The hybrid fit agrees well with that to the head-on collision data in the entire available energy range. For the centrality data, the power-law ε_{NN}-fit is also found to be very close to the power-law $\sqrt{s_{NN}}$-fit of the head-on collision data.

From this one concludes that within the picture proposed here the data are well reproduced under the assumption of the effective energy deriving the multiparticle production process and pointing to the the same energy behaviour of all types of heavy-ion collisions, from peripheral to the most central collisions. This observation is similar to that obtained by us earlier [2] for the midrapidity pseudorapidity density and the transverse energy density data at midrapidity.

From the hybrid fits obtained, we estimate the multiplicity for the future LHC heavy-ion run. Since the hybrid fit for head-on collision data and the fit to the centrality data show slightly different increase with c.m. energy, the predictions of the two fits are averaged. Hence, the mean multiplicity $2N_{\rm ch}/N_{\rm part}$ value is predicted to be about 128 within 5% uncertainty in the most central heavy-ion collisions at $\sqrt{s_{NN}} = 5.52$ TeV. The prediction is shown by the right-inclined hatched area in Fig. 1. In addition, the fit-averaged prediction based on pp collisions at $\sqrt{s_{pp}} = 14$ TeV, being recalculated within the participant dissipating energy approach, is shown in Fig. 1 as the left-inclined hatched area. Similarly to the existing data on the mean multiplicity $N_{\rm part}$-dependence, the head-on data hybrid fit is used to make the predictions for the centrality dependence to be measured in the forth-

coming heavy-ion collisions at $\sqrt{s_{NN}} = 5.52$ TeV. The predictions are shown by the dashed-dotted line in Fig. 2, where the centrality and $N_{\rm part}$ values are alike in the 2.76 TeV data shown. The expectations show increase of the mean multiplicity with $N_{\rm part}$ (decrease with centrality) from about 83 to about 132. The increase looks to be slightly faster than at $\sqrt{s_{NN}} = 2.76$ TeV, especially for the peripheral region. One can see that, except a couple of ponts from peripheral collisions, the predictions are well reproduced by the LHC data, when the latter are scaled by a factor of 1.47.

8. In summary, the multihadron production process in nucleus-nucleus collisions and its universality in nuclear and hadronic interactions are studied using the charged particle mean multiplicity dependencies on the c.m. collision energy per nucleon, $\sqrt{s_{NN}}$, and on the number of nucleon participants, or centrality, measured in the energy range of a few GeV to a few TeV. The study is carried out in the framework of the earlier proposed participant dissipating energy approach [3, 4]. In this approach, the participants are considered to form the initial zone of a collision and to determine the production of hadrons at the very early stage of the collision. In this consideration one combines the constituent quark picture with Landau hydrodynamics and interrelates the multihadron production in different types of collisions by proper scaling of the c.m. energy of collisions. In particular, an energy-scaling factor of 1/3 in $pp/\bar{p}p$ measurements is shown to reveal the universality of the multiplicity dependencies in nucleon-nucleon and nucleus-nucleus interactions.

In the entire available $\sqrt{s_{NN}}$ range of about a few TeV, the energy dependence of the multiplicity in head-on collisions is found to be well described by the calculations performed within the effective-energy approach based on $pp/\bar{p}p$ data. Meanwhile, depending on the data sample, the calculations are found either to describe the measured centrality dependence or to show some deviation between the calculations and the data. For the RHIC data, the deficit in the predictions is observed for non-central collisions so that the predictions do not follow a constancy with the centrality as it is observed at RHIC. In contrary, the LHC mean multiplicity centrality dependence is found to be well described by the calculations: both the data and the calculations showing an increase towards the most central collisions.

To clarify on the observations, the quark participant effective-energy approach is applied to the pseudorapidity density distribution measured in heavy-ion collisions. The energy balanced limiting fragmentation scaling is introduced under assumption of the similarity of the fragmentation region of the measured distribution in the beam rest frame and that determined from the calculations by using the effective energy. The revealed scaling allows to reproduce the pseudorapidity density distributions independent of the centrality of collisions and then to correctly describe the centrality independence of the mean multiplicity obtained at RHIC. Moreover, this finding provides a solution of the RHIC "puzzle" of the difference between the centrality independence of the mean multiplicity *vs.* the monotonic decrease of the midrapidity pseudorapidity density with the increase of centrality.

Based on the above findings, the complementarity of the head-on collisions and the centrality data is shown resulting in the similar energy behaviour of the mean multiplicity measurements as soon as the data are considered in terms of the effective energy. A departure of the c.m. energy dependence of the data from the logarithmic behaviour to the power-law one observed at around 1 TeV points to an apparent transition to a new regime in nucleus-nucleus collisions at TeV energies.

The predictions for the charged particle mean multiplicity in head-on heavy-ion collisions at

$\sqrt{s_{NN}} = 5.52$ TeV at the LHC are given. Within the obtained complementarity of head-on collisions and centrality data, the predictions are also made for the mean multiplicity centrality dependence.

References

[1] For review, see: W. Kittel, E.A. De Wolf, *Soft Multihadron Dynamics* (World Scientific, Singapore, 2005)

[2] A.N. Mishra, R. Sahoo, E.K.G. Sarkisyan, A.S. Sakharov, *Eur. Phys. J. C* **74** (2014) 3147

[3] E.K.G. Sarkisyan, A.S. Sakharov, *Eur. Phys. J. C* **70** (2010) 533

[4] E.K.G. Sarkisyan, A.S. Sakharov, *AIP Conf. Proc.* **828** (2006) 35

[5] E.K.G. Sarkisyan, A.N. Mishra, R. Sahoo, A.S. Sakharov, arXiv:1506:0908

[6] L.D. Landau, *Izv. Akad. Nauk: Ser. Fiz.* **17** (1953) 51. English translation: *Collected Papers of L. D. Landau*, ed. by D. Ter-Haarp (Pergamon, Oxford, 1965), p. 569.

[7] See *e.g.* P. Steinberg, *J. Phys. Conf. Ser.* **9** (2005) 280

[8] For review and a collection of reprints on original papers on quarks and composite models, see: J.J.J. Kokkedee, *The Quark Model* (W.A. Benjamin, Inc., New York, 1969)

[9] V.V. Anisovich, N.M. Kobrinsky, J. Nyiri, Yu.M. Shabelsky, *Quark Model and High Energy Collisions* (World Scientific, Singapore, 2004)

[10] See *e.g.* R. Rougny (for the CMS Collab.), *Nucl. Phys. B (Proc. Suppl.)* **207-208** (2010) 29

[11] The Review of Particle Physics, K.A. Olive *et al.* (Particle Data Group), Chin. Phys. C **38**, 090001 (2014).

[12] G. Wolschin, *J. Phys. G* **40** (2013) 045104

[13] R. Sahoo, A.N. Mishra, N.K. Behera, B.K. Nandi, *Adv. High Energy Phys.* **2015** (2015) 612390

[14] J.F. Grosse-Oetringhaus, K. Reygers, *J. Phys. G* **37** (2010) 083001

[15] CMS Collab., S. Chatrchyan *et al.*, *J. High Energy Phys.* **08** (2011) 141

[16] B. Alver *et al.*, *Phys. Rev. C* **83** (2011) 024913

[17] ALICE Collab., E. Abbas *et al.*, *Phys. Lett. B* **726** (2013) 610

[18] A. Toia (for the ALICE Collab.), *J. Phys. G* **38** (2011) 124007

[19] UA5 Collab., G.J. Alner *et al.*, *Z. Phys. C* **33** (1986) 1

[20] J. Benecke, T.T. Chou, C.N. Yang, E. Yen, *Phys. Rev.* **188** (1969) 2159

[21] C.-Y. Wong, *Phys. Rev. C* **78** (2008) 054902

[22] A. Sen, J. Gerhard, G. Torrieri, K. Read, C.-Y. Wong, *Phys. Rev. C* **91** (2015) 024901